

# An Economic Model Predictive Control Approach for Load Mitigation on Multiple Tower Locations of Wind Turbines

Zhixin Feng, Alexander J. Gallo, Yichao Liu, Atindriyo K. Pamososuryo,  
Riccardo M.G. Ferrari and Jan-Willem van Wingerden

**Abstract**—The current trend in the evolution of wind turbines is to increase their rotor size in order to capture more power. This leads to taller, slender and more flexible towers, which thus experience higher dynamical loads due to the turbine rotation and environmental factors. It is hence compelling to deploy advanced control methods that can dynamically counteract such loads, especially at tower positions that are more prone to develop cracks or corrosion damages. Still, to the best of the authors’ knowledge, little to no attention has been paid in the literature to load mitigation at multiple tower locations. Furthermore, there is a need for control schemes that can balance load reduction with optimization of power production. In this paper, we develop an Economic Model Predictive Control (eMPC) framework to address such needs. First, we develop a linear modal model to account for the tower flexural dynamics. Then we incorporate it into an eMPC framework, where the dynamics of the turbine rotation are expressed in energy terms. This allows us to obtain a convex formulation, that is computationally attractive. Our control law is designed to avoid the “turn-pike” behavior and guarantee recursive feasibility. We demonstrate the performance of the proposed controller on a 5MW reference WT model: the results illustrate that the proposed controller is able to reduce the tower loads at multiple locations, without significant effects to the generated power.

## I. INTRODUCTION

Wind energy has recently received increasing attention in the international energy market. In 2020, 90 GW of new wind power capacity was deployed, contributing to a global growth of 53% compared to 2019 [1]. Such growth is partially driven by the increasing physical dimension of wind turbines (WTs), which allows for more wind power to be captured. However, higher fatigue loads on the increasingly flexible WT towers are also experienced as a downside of this trend. Extra attention, therefore, needs to be paid to mitigate the structural loads while keeping power production minimally affected, as these objectives are often competitive. From the control engineering standpoint, this urges for the employment of advanced controllers, capable of addressing the power regulation and load mitigation trade-off.

In the literature, a number of control algorithms that are able to cater for the aforementioned trade-off have been pro-

posed. For instance, a quasi-linear parameter varying model predictive control scheme was used in [2] and an adaptive gain scheduling proportional–integral (PI) control was proposed in [3]. In addition, the economic model predictive control (eMPC) framework was proposed to optimize the aforementioned trade-off [4], [5]. eMPC is a control paradigm that has been introduced in the past decade to include economic considerations in the objective function of predictive controllers, rather than tracking reference points [6]. The control methods mentioned above mainly account for fatigue loads at the tower bottom location. However, critical damage can be caused by fatigue loads on other tower locations as well, where cracks or serious corrosion can occur. Thus, the reduction of fatigue loads at more than one location along the WT’s tower is of importance. Still, to the best of the authors’ knowledge, there are no contributions in literature addressing the design of a controller capable of optimizing the trade-off of power generation and the reduction of loads at multiple tower locations. Additionally, *turnpike* behavior is a common feature of finite-horizon eMPC [6], [7]. This undesired behaviour refers to the fact that the optimizer may drive the nominal system away from the optimal steady state at the end of the prediction horizon. Although addressed in [8] by including a suitably defined term in the objective function of the eMPC-based controller, analysis of appropriate solutions to avoid the turnpike behavior is lacking from a large number of works in the literature addressing eMPC for WTs.

In this paper, we develop an eMPC-based controller that simultaneously reduces loads at multiple WT tower locations and maximizes power generation. Our main contributions are

- we leverage modal analysis to include a higher order approximation of the tower fore-aft flexural dynamics [9];
- we improve performance by introducing a terminal constraint in the eMPC law, based on the optimal steady state, which avoids the turn-pike behavior;
- we apply the proposed controller to the National Renewable Energy Laboratory (NREL)’s 5MW reference WT model [10] and present the extensive results.

The higher order flexural model allows us to predict the state of the WT more accurately, thus achieving higher performance with respect to existing control strategies. Additionally, the inclusion of a terminal constraint ensures that optimal trajectories do not exhibit *turnpike* behavior, while also improving control performance. The effectiveness of the proposed controller is compared to other eMPC-based solutions from the literature, specifically: one with

This work is partially supported by the WATEREYE project, which is funded by European Innovation and Networks Executive Agency under the European Union’s Horizon 2020 research and innovation program under grant agreement no. 851207, and was also supported by the AIMWIND project, funded by the Research Council of Norway under grant no. 312486.

Authors are with the Delft Center for Systems and Control, Delft University of Technology, Mekelweg 2, 2628 CD Delft, The Netherlands. {Z.Feng-2, A.J.Gallo, Y.Liu-17, A.K.Pamososuryo, R.Ferrari, J.W.vanWingerden}@tudelft.nl.

single-location tower load reduction [4], and one in which tower loads are not included in the controller objective function [11]. Analysis of the effects of the prediction horizon length is also given, highlighting the need to balance performance and computational complexity. In this respect, we note how including a terminal constraint further improves performances at a negligible computational cost.

The remainder of this paper is organized as follows: in Section II the system dynamic model is defined. Section III formalizes the eMPC framework for loads reduction on multiple tower locations. In Section IV, case studies are carried out to numerically demonstrate the proposed controller. Finally, conclusions are drawn in Section V.

## II. DEFINITION OF THE SYSTEM DYNAMIC MODEL

Let us start by introducing the dynamical model of the WT used in this paper; specifically, we utilize a single rotational model to describe the dynamics of the turbine drive train, and a multi-mode model to approximate the tower vibration.

### A. Drive Train Dynamics

Let  $\omega_g$  denote the generator angular speed. Then the single-order model of the drive train dynamics is formulated as:

$$\dot{\omega}_g = \frac{1}{J} \left[ \frac{1}{G} T_r - T_g \right], \quad (1)$$

where  $T_r$ ,  $T_g$  and  $G \geq 1$  are the rotor torque, generator torque and gearbox ratio, respectively;  $J = J_g + J_r/G^2$  represents the equivalent inertia at the generator shaft, where  $J_r$  and  $J_g$  are, respectively, the rotor and generator inertia; and, supposing a stiff rotor shaft, the rotor speed is  $\omega_r = \omega_g/G$ . The rotor torque  $T_r$  is defined by:

$$T_r = \frac{1}{2\omega_r} \rho A C_p(\lambda, \beta) v_w^3, \quad (2)$$

where  $\rho$  is the air density;  $A$  is the rotor swept area;  $\beta$  is the blade pitch angle;  $v_w$  is the wind speed; and  $\lambda$  represents the tip-speed ratio, defined as:

$$\lambda = \frac{\omega_r D_r}{2v_w} = \frac{\omega_g D_r}{2Gv_w}, \quad (3)$$

where  $D_r$  is the rotor diameter. Finally,  $C_p$  is the nonlinear power coefficient, specific to each WT, which is derived via experiments or steady-state simulations. For the NREL's 5MW WT [10] considered in this work, look-up tables for  $C_p$  have been derived for control design.

The aerodynamic power extracted from the wind,  $P_r$ , and the generator power,  $P_g$ , are defined as:

$$P_r = T_r \omega_r = \frac{1}{2} \rho A C_p(\lambda, \beta) v_w^3, \quad (4)$$

$$P_g = \eta_g T_g \omega_g, \quad (5)$$

where  $\eta_g$  is the generator efficiency. As is standard in this modeling framework, we consider  $\omega_g$  as the state variable of the system, while  $\beta$  and  $T_g$  are controllable inputs, and  $v_w$  is an uncontrolled input to the system.

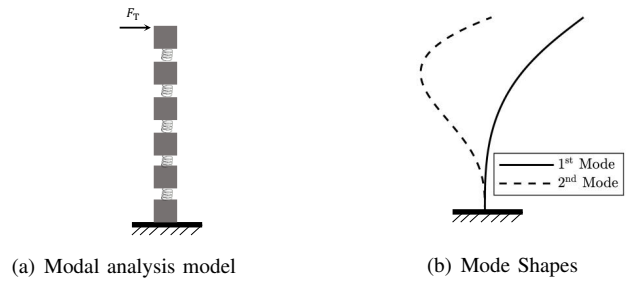


Fig. 1. Tower vibration model and its mode shapes

For proper operation of the WT, the following state, input, and output constraints must be guaranteed [11]:

$$\omega_{g,\min} \leq \omega_g \leq \omega_{g,\max}, \quad (6)$$

$$0 \leq T_g \leq T_{g,\max}, \quad (7)$$

$$\beta_{\min} \leq \beta \leq \beta_{\max}, \quad (8)$$

$$0 \leq P_g \leq P_{g,\text{rated}}. \quad (9)$$

### B. Multi-mode Tower Vibration Model

Having presented the dynamical model of the WT drive train, let us now define our modeling of the WT tower vibrations. Specifically, we are interested in the tower fore-aft vibrations.

Let  $F_T$  denote the thrust force. As shown in Fig. 1(a), the tower structure can be modeled as a multiple mass-spring-damper system which is fixed at the bottom. Here we approximate the tower vibration dynamics via modal analysis [9], through which the vibration can be decomposed into different contributing modes. In Fig. 1(b) we show the mode shapes of the first two contributing modes. Let  $\Phi \in \mathbb{R}^{N_d \times N_m}$  represent the mode-shape matrix, with  $\Phi_i = [\phi_{1,i}, \dots, \phi_{N_d,i}]^T$  being the  $i^{\text{th}}$  column of the matrix and  $N_d$  the number of degrees of freedom. Let then  $N_l$  denote the number of locations: then  $z_l \in [0, 1]$ ,  $l \in \{1, \dots, N_l\}$  represent the *normalized* heights, with  $z_1 = 1$ . To exploit the modeling modal framework, we must be able to relate  $\mathbf{x}_p = [x_{p,1}, \dots, x_{p,N_l}]^T$ , the physical displacement of the tower locations, to a modal displacement  $\mathbf{x}_m \in \mathbb{R}^{N_m}$ . Here,  $N_m$  is the number of contributing modes considered. According to the order-reduction analysis [12],  $\mathbf{x}_p$  can be expressed as:

$$\mathbf{x}_p = \mathbf{S}^T \mathbf{x}_m, \quad (10)$$

where  $\mathbf{S} = [s_{il}] \in \mathbb{R}^{N_m \times N_l}$  is a matrix in which each element  $s_{il}$  represents the shape of the  $i^{\text{th}}$  mode at height  $z_l$ . Such elements are defined as:

$$s_{il} = \Phi_i^T [z_l^0 \quad \dots \quad z_l^{N_d-1}]^T. \quad (11)$$

The multi-mode tower vibration model [9] can be then described compactly as:

$$\ddot{\mathbf{x}}_m + \mathbf{M}_m^{-1} \mathbf{D}_m \dot{\mathbf{x}}_m + \mathbf{M}_m^{-1} \mathbf{K}_m \mathbf{x}_m = \mathbf{B}_m F_T, \quad (12)$$

where the diagonal matrices  $\mathbf{M}_m$ ,  $\mathbf{K}_m$ ,  $\mathbf{D}_m \in \mathbb{R}^{N_m \times N_m}$  are, respectively, the modal mass, stiffness and damping matrices. Specifically, each diagonal element  $m_{m,i}$  of  $\mathbf{M}_m$  is defined

as [13], [14]:

$$m_{m,i} = \sum_{l=1}^{N_d} \rho(z_l) s_{il}^2 \Delta z_l H_t, \quad (13)$$

where  $H_t$  is the tower height;  $\rho(z_l)$  is the tower mass density at height  $z_l$ ; and  $\Delta z_l = z_l - z_{l-1}$ . The diagonal elements of  $\mathbf{D}_m$  and  $\mathbf{K}_m$  are assumed to be given. The matrix  $\mathbf{B}_m \in \mathbb{R}^{N_m}$  is the input matrix in modal analysis coordinate, defined as  $\mathbf{B}_m = \mathbf{M}_m^{-1} \Phi^\top \mathbf{B}_o$  [9]. The symbol  $\mathbf{B}_o = [1 \quad \mathbf{0}^{1 \times N_d-1}]^\top$  indicates that the aerodynamic thrust force  $F_T$  is applied at the top of the tower, as shown in Fig. 1(b). Finally  $F_T$ , which is the input to (12), is calculated as:

$$F_T = \frac{1}{2} \rho A C_t(\lambda, \beta) v_w^2, \quad (14)$$

where  $C_t$  is the thrust coefficient, a nonlinear function of  $\lambda$  and  $\beta$ , and is dependent on the physical characteristics of the turbine. Similar to  $C_p$ ,  $C_t$  can be derived and stored in a look-up table for control purposes.

### III. EMPC TOWER DAMPING CONSIDERING MULTIPLE VIBRATION MODES

Having presented the WT model, let us now introduce the eMPC-based controller to simultaneously reduce fatigue loads on multiple tower locations. Given the nonlinear nature of the WT dynamics defined in Section II, we start by presenting a method to linearize them via a change of variables, introduced in [4], [11]; following this, we mathematically formulate the objective function for tower load reduction; finally, we define the full eMPC-based controller.

#### A. Convex Constraints Formulation

To simplify the analysis of the eMPC-based controller, the nonlinear model of the WT can be made linear by introducing the *kinetic energy*, while keeping the constraints convex [4], [11]. The kinetic energy  $K$  stored in the generator is defined as:

$$K = \frac{J}{2} \omega_g^2. \quad (15)$$

By substituting (15) into the drive train dynamics defined in (1), dynamics of  $K$  is derived as:

$$\dot{K} = J \omega_g \dot{\omega}_g = \omega_g \left( \frac{1}{G} T_r - T_g \right) = P_r - \frac{1}{\eta_g} P_g. \quad (16)$$

Here, the introduction of  $P_r$  and  $P_g$ , considered as directly controllable inputs, allows for a linear formulation of the dynamics.

Finally, to complete the linearization of the dynamics, we must ensure that the modal dynamics in (12) are linear with respect to the kinetic energy [4]. To do this, we define the following approximation of the thrust force:

$$\hat{F}_T = \zeta_1 P_r + \zeta_2 K + \zeta_3, \quad (17)$$

where  $\zeta_1, \zeta_2, \zeta_3 \in \mathbb{R}$  are derived from the linearization of (14) around an operating point. By defining  $\mathbf{v}_m = \dot{\mathbf{x}}_m$ , we have:

$$\dot{\mathbf{v}}_m = \mathbf{M}_m^{-1} \left[ \Phi^\top (\zeta_1 P_r + \zeta_2 K + \zeta_3) - \mathbf{D}_m \mathbf{v}_m - \mathbf{K}_m \mathbf{x}_m \right]. \quad (18)$$

Hence, a state space representation of the turbine dynamics can be defined as:

$$\dot{\mathbf{x}}(t) = \mathbf{A} \mathbf{x} + \mathbf{B} \mathbf{u}(t), \quad (19)$$

where  $\mathbf{x} = [K, \mathbf{x}_m^\top, \mathbf{v}_m^\top]^\top \in \mathbb{R}^{2N_m+1}$ ,  $\mathbf{u} = [P_r, P_g]^\top \in \mathbb{R}^2$ , and  $\mathbf{A}$  and  $\mathbf{B}$  are derived from (16) and (18).

We now show that the constraints (6)-(8) remain convex. Given the definition of  $K$  in (15), the state constraints expressed in (6) can be rewritten as:

$$\frac{J}{2} \omega_{g,\min}^2 \leq K \leq \frac{J}{2} \omega_{g,\max}^2, \quad (20)$$

Moreover, the input constraints (7)-(8) can be rewritten for  $P_r$  and  $P_g$  as:

$$\begin{cases} 0 \leq P_r \leq \hat{P}_{av}(v_w, K) \\ 0 \leq P_g \leq \eta_g T_{g,\max} \sqrt{\frac{2}{J} K} \end{cases}, \quad (21)$$

where  $\hat{P}_{av}(v_w, K)$  is a convex approximation of  $P_{av}(v_w, K)$ , the available wind power. Similarly, the physical bound of  $\hat{F}_T$  as defined in (17) must satisfy:

$$0 \leq \hat{F}_T \leq F_{T,\max}, \quad (22)$$

where  $F_{T,\max}$  is the maximum thrust force, given  $v_w$  and  $K$ , as defined in [4], i.e.

$$F_{T,\max} = \max_{\beta_{\min} \leq \beta \leq \beta_{\max}} 0.5 \rho A C_t(K, \beta) v_w^2. \quad (23)$$

In conclusion, a convex constraint function  $C(\mathbf{x}, \mathbf{u})$ , to be used in eMPC, can be constructed such that  $C(\mathbf{x}, \mathbf{u}) \leq 0$  ensures that (20), (21) and (22) hold.

#### B. Load reduction at multiple tower locations

The objective of our proposed controller is to reduce the fatigue loads at multiple locations. Let us start by introducing the *Tower Fore-Aft Moment* (TFAM) at location  $z_l$  of the tower. The cyclic loads, i.e., the variation of TFAM( $z_l$ ) over time [15] and at multiple heights  $z_l, l \in \{1, \dots, N_l\}$  are taken into account as they are related to fatigue accumulation:

$$\begin{aligned} \frac{d}{dt} \text{TFAM}(z_l) &= (H_t - z_l) (d_l (\ddot{x}_{p,\text{top}} - \ddot{x}_{p,l}) \\ &\quad + k_l (\dot{x}_{p,\text{top}} - \dot{x}_{p,l})), \end{aligned} \quad (24)$$

where  $x_{p,\text{top}} = H_t$ , and  $d_l, k_l$  are the damping and stiffness coefficients, which are constant for  $z_l$ . Such loads can be effectively reduced by minimizing the term  $\dot{x}_{p,\text{top}} - \dot{x}_{p,l}$  [4]. Let  $\mathbf{v}_p = \dot{\mathbf{x}}_p$ . Since the loads at the tower base are the highest,  $v_{p,\text{bottom}} = 0$  must be included in  $\mathbf{v}_p$ . As a proxy for minimizing the TFAM, we will here minimize  $\mathbf{v}_p$ , by assigning a larger weight for minimizing  $v_p$  (details are explained in Section IV-B). With (10) in mind, we can thus define the following objective

$$O_v = \mathbf{v}_p^\top \mathbf{W} \mathbf{v}_p = \mathbf{v}_m^\top \mathbf{S} \mathbf{W} \mathbf{S}^\top \mathbf{v}_m \quad (25)$$

where  $\mathbf{W} = \text{diag}_{i \in \{1, \dots, N_l\}} [w_i]$  are weights allowing to account for the relative importance of multiple tower locations.

### C. Load-limiting eMPC

We are now ready to present the eMPC-based controller to achieve power maximization with tower load limiting at multiple locations.

As discussed in Section III-A, the WT dynamics can be described as the linear system in (19), and a convex constraint  $C(\mathbf{x}, \mathbf{u}) \leq 0$  can be defined. In addition, we include in  $C(\mathbf{x}, \mathbf{u})$  the following

$$0 \leq K \leq \frac{J}{2} \omega_{g, \text{rated}}^2 + \epsilon, \quad (26)$$

where  $\epsilon$  is a variable in the objective function, used to limit the turbine's oversping, as is further detailed in the following.

Finally, before moving on to the definition of the eMPC-based controller, let us define its objective function. We consider a scalar weighted sum of multiple objectives, where the weights are defined such that appropriate tradeoffs between conflicting goals can be achieved. Specifically, we define

$$O(\mathbf{x}, \mathbf{u}) \doteq \alpha_1 P_g + \alpha_2 \hat{P}_{\text{av}}(v_w, K) - \alpha_3 \dot{P}_g^2 - \alpha_4 \dot{P}_r^2 - \alpha_5 \epsilon - O_v(\mathbf{x}), \quad (27)$$

where  $\alpha_\gamma, \gamma \in \{1, \dots, 5\}$  are appropriately defined weights, to be tuned together with  $w_l, l \in \{1, \dots, N_l\}$ . When maximizing the objective function  $O(\mathbf{x}, \mathbf{u})$ , the first terms in  $P_g$  and  $\hat{P}_{\text{av}}$  determines the maximization of the power output of the turbine. Next two terms penalize their rate of change, while the fifth one penalizes the turbine's deviation from its rated rotational speed. Finally, the last term minimizes the velocity of the displacement at  $N_l$  tower locations, and thus the TFAM.

In line with standard formulation of model predictive control, the control law is formulated as a *Finite-Horizon Optimal Control Problem* (FHOCP):

$$\max_{\mathbf{U}, \epsilon} \sum_{q=0}^{N_p-1} O(\bar{\mathbf{x}}(q), \mathbf{u}(q)), \quad (28a)$$

$$\text{s.t. } \bar{\mathbf{x}}(q+1) = A_d \bar{\mathbf{x}}(q) + B_d \mathbf{u}(q), \quad (28b)$$

$$C(\bar{\mathbf{x}}(q), \mathbf{u}(q)) \leq 0, \forall q \in \{0, \dots, N_p - 1\}, \quad (28c)$$

$$\bar{\mathbf{x}}(0) = \mathbf{x}(t_k), \quad (28d)$$

$$\bar{\mathbf{x}}(N_p) = \mathbf{x}_s, \quad (28e)$$

where  $N_p$  is the finite horizon,  $\bar{\mathbf{x}}(q) = [\bar{K}(q), \bar{\mathbf{x}}_m^\top(q), \bar{\mathbf{v}}_m^\top(q)]^\top, q \in \{0, \dots, N_p\}$  is the predicted state of the system at time instant  $q$ ,  $(A_d, B_d)$  are the result of discretization of (19) with a sampling time  $T_s$ .  $\mathbf{x}(t_k)$  is the state at time  $t_k$ , which is reconstructed from the measurements  $\omega_g(t_k), \mathbf{x}_p, \mathbf{v}_p$  based on (15) and (10). and  $\mathbf{U} = [\mathbf{u}^\top(0), \dots, \mathbf{u}^\top(N_p - 1)]^\top \in \mathbb{R}^{2N_p}$ .

The constraints of the FHOCP are defined as follows: (28b) represents the dynamics with which the state is predicted, (28c) guarantees that the constraints are satisfied, (28d) sets the initial state of the nominal model to be the same as the measured state at time  $t_k$ . (28e) is a terminal constraint on the predicted state, which ensures that the

terminal predicted state is the same as  $\mathbf{x}_s$ , the optimal steady-state state. This is calculated by solving:

$$\begin{aligned} \max_{\mathbf{x}_s, \mathbf{u}_s} \quad & O(\mathbf{x}_s, \mathbf{u}_s) \\ \text{s.t.} \quad & \mathbf{x}_s = A_d \mathbf{x}_s + B_d \mathbf{u}_s \\ & C(\mathbf{x}_s, \mathbf{u}_s) \leq 0 \end{aligned} \quad (29)$$

The terminal constraint (28e) is included in the FHOCP, to ensure that the optimal trajectories over the prediction horizon do not exhibit *turnpike* behavior, and ensures recursive feasibility of the FHOCP (28).

The solution to (28) is computed at every time step  $t_k$ , the optimal value  $\mathbf{U}^*$  is found, and  $\mathbf{u}(t_k) = \mathbf{u}^*(0)$  is applied to the system. For each of the following time instants, the problem (28) will roll ahead and the procedure is repeated at the next time instant. In the proposed scheme the model was transformed resulting in linear dynamics, and convex constraints and a concave objective function are derived. Therefore, the problem can be solved globally and in a computationally efficient way [16].

Since the dynamics and constraints of the FHOCP are formulated in power and energy variables as detailed in Section III-A, it is necessary for  $\mathbf{u}(t_k)$  to be translated back into the original, usable WT control signals, namely  $T_g^* = P_g / (\eta_g \sqrt{2K^*/J})^1$  and  $\beta^* = \Psi(P_r^*, v_w, K^*)$ . The pitch look-up table  $\Psi$  contains the inverse nonlinear mapping involving  $C_p$ , only defined for the pitch range (8). Thus, it is ensured that  $\beta$  will not violate its operational bounds.

## IV. SIMULATION RESULTS AND ANALYSIS

In this section, the performance of the proposed eMPC approach is demonstrated on a simplified NREL's 5MW WT dynamic model. The eMPC-based controller proposed in Section III with a two-mode model of the tower vibration dynamics is compared to two eMPC-based controllers in literature: one with single mode damping, proposed in [4], and one without tower damping, designed in [11].

### A. Turbine Configuration

The natural frequency of the first and second mode are 0.3240 Hz and 2.9003 Hz, respectively. Other structural and dynamic model parameters, such as the tower mass and damping ratio, can be found in [10].

Without loss of generality, two tower measurements considered in the case study to illustrate the load mitigation performance: i. the tower top ( $z_1 = 1$ ) where the dominant displacement occur, and ii. the location ( $z_2 = 0.72$ ) where the maximum displacement of the second mode shape is observed. In practice, other tower locations where the measurement device is instrumented can be selected for load reduction, depending on the user's need.

<sup>1</sup>With a slight abuse of notation,  $K^*$  here represents the one-step ahead prediction of  $K$ .

## B. Simulation Configuration

A uniform wind flow, whose velocity follows a staircase profile, is considered. The stepwise wind speed increases from 6 to 17 m/s, with each step lasting for 100 s. The weights  $\alpha_\gamma$  ( $\gamma = \{1, \dots, 5\}$ ) and  $w_l, l = \{1, 2\}$  are tuned to find a suitable trade-off between power regulation and tower loads reduction. For  $\alpha_\gamma$ , the weights are selected to guarantee each term with the same order of magnitude. While designing  $w_l$ , we focus more on the tower bottom load-reduction because it is the location where the strongest fatigue loads are suffered. Thus, we choose  $w_1 - w_2 > 2w_2$  to guarantee the proxy mentioned in Section II-B. Besides,  $w_l$  can not be too large because we do not want to sacrifice too much generated power. Based on the rules explained above, we choose the weights presented in Table I.

The simulation platform is MATLAB/Simulink software. The computer configuration is a laptop with a CPU i7-8665U, 2.11 GHz frequency and a 8 GB memory capacity. The sampling time of the simulation is 0.2 s. Regarding the definition of the prediction horizon, we remark that this should be chosen as a compromise between the computational time required to solve (28) and system performance. To demonstrate this trade-off, we compare three different values of  $N_p$ : a.  $N_p = 50$ , b.  $N_p = 100$ , c.  $N_p = 200$ . The results of this comparison are shown in Fig. 2, from which it is found that the controller with  $N_p = 100$  shows similar performance to the one with  $N_p = 200$ , but at lower computation cost. Therefore,  $N_p = 100$  is selected for the comparison study, implying a 20s prediction horizon.

TABLE I  
WEIGHTS IN OBJECTIVE FUNCTION

$\alpha_1$	$\alpha_2$	$\alpha_3$	$\alpha_4$	$\alpha_5$	$w_1$	$w_2$
1	1	1	0.01	100	100	20

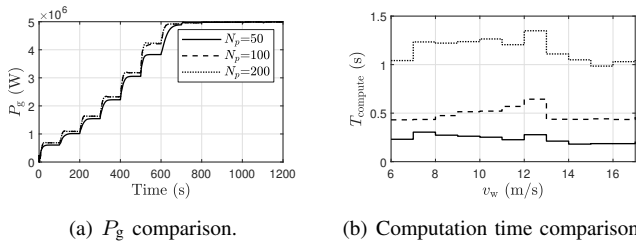


Fig. 2. Comparison of  $N_p = 50$ ,  $N_p = 100$ ,  $N_p = 200$ .

## C. Controller Performance

First, the trajectories of the velocities and accelerations are presented in Figs. 3 and 4. It shows that the structural load at both locations is alleviated by the two-modes-damping control strategy: indeed, the amplitude and oscillation of the velocities of both locations are significantly reduced. With (24) in mind, this leads to the fatigue loads at both locations being alleviated. Furthermore, Fig. 5 illustrates the performance of the power generation. In Figs. 5(a) and 5(b), at  $v_w = 7$  m/s and 10 m/s,  $P_g$  at steady states stays the same.

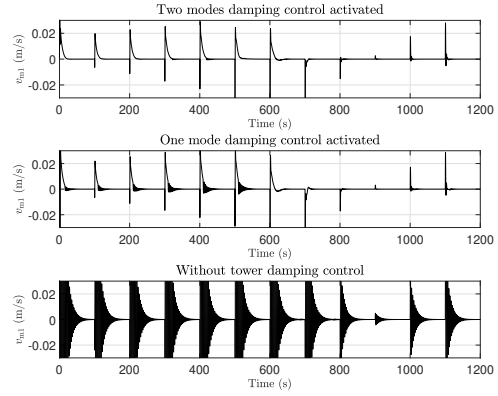


Fig. 3. Comparison of  $v_1$  on location  $z_1 = 1$ .

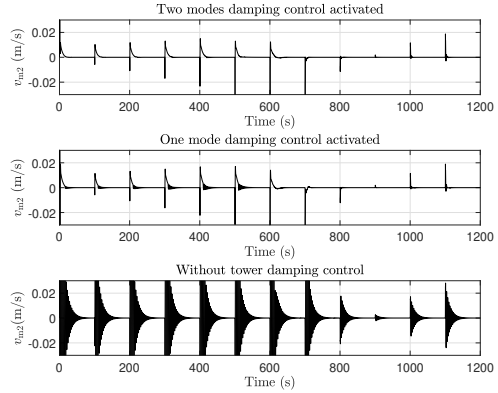


Fig. 4. Comparison of  $v_2$  on location  $z_2 = 0.72H_t$ .

In Figs. 5(c) and 5(d), at  $v_w = 14$  m/s and 17 m/s, there is a minor power loss around 0.5%, which can be considered as negligible impacts on the power generation. The power generation at other wind speeds are similar, which is omitted for brevity. In summary, a small amount of  $P_g$  is sacrificed for tower load-reduction at above-rated wind speeds, while there is no power loss introduced by the proposed load-limiting control at below-rated wind speeds. Therefore, it is concluded that the proposed eMPC-based controller performs efficient load reduction at multiple tower locations, without significant effects on the power regulation.

## D. The Importance of Terminal Constraints

As discussed in Section III, to reduce the turnpike phenomenon, we construct terminal constraints for the states  $\bar{x}(N)$  (28e). In Fig. 6(a)-6(b), we show the optimal trajectory of the nominal states  $\bar{K}$  and  $\bar{v}_{m,1}$ , i.e., the first and third components of the nominal state  $\bar{x}$ , over one prediction horizon, with and without terminal conditions. From this, it can be seen that the turnpike effect is significantly reduced. Similar results can be found for  $x_{m1}, x_{m2}$  and  $v_{m2}$ .

Apart from the reduction in the turnpike behavior over the prediction horizon, in Fig. 6(c)-6(d) we show how the inclusion of the terminal constraint (28e) improves the controller performance. Indeed, in Fig. 6(c) we show that, at above rated wind speed  $v_w = 16$  m/s, the  $P_g$  resulting from the controller with a terminal constraint is larger than

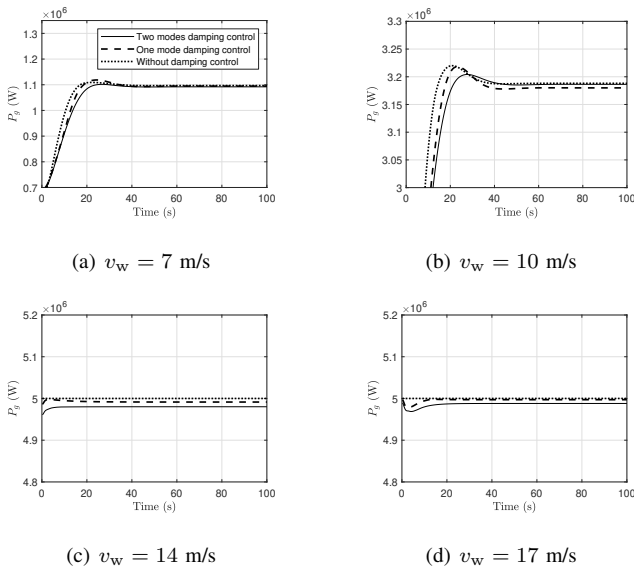


Fig. 5. Comparison of  $P_g$  at different wind speeds.

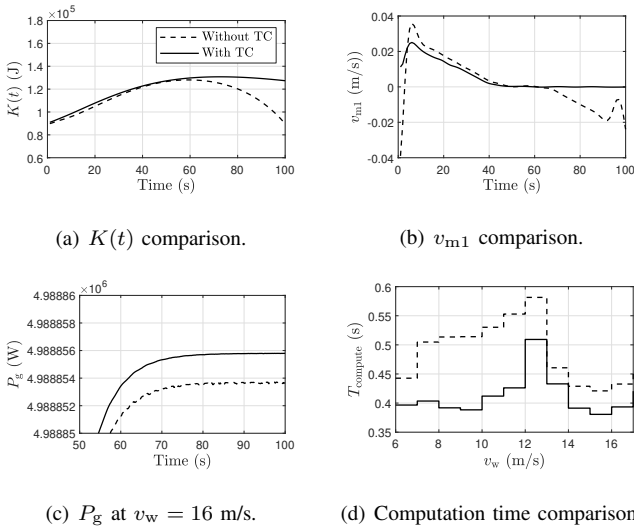


Fig. 6. Comparison of performance between the eMPC-based controllers with and without terminal constraints

the case without (28e). Furthermore, in Fig. 6(d) we see that there is a reduction of computation time for the solution of the FHOCP with the terminal constraint compared to the FHOCP without (28e), across a wide range of wind speeds.

## V. CONCLUSIONS

In this paper, we develop a load-limiting control based on the economic model predictive control (eMPC) framework to mitigate tower fatigue loads on multiple locations of wind turbines (WTs). In detail, a multi-mode vibration model is first incorporated into the eMPC framework, which allows for load reduction on multiple tower locations. Secondly, the rotational dynamics of the WT are written in energy terms, allowing to obtain a linear eMPC problem with convex constraints. Finally, a simulation study is performed to illustrate the scheme effectiveness, and analyse the influence of different prediction horizons and of terminal constraints. To eval-

uate the control performance of the proposed approach, also eMPC-based controllers without tower damping and with one mode damping only are implemented for comparison. Simulation results show that the proposed controller is able to effectively reduce the vibration at multiple locations, without significant effects on the power generation. In addition, the terminal constraints in the eMPC framework shows good effectiveness in alleviating the turnpike behavior.

In future work, we will further verify the proposed controller using a high-fidelity WT model, such as Fatigue, Aerodynamics, Structures, and Turbulence (FAST). Furthermore, the current controller can be extended for floating WT's considering tower model with multiple degrees of freedom.

## REFERENCES

- [1] "Global wind report 2021," Global Wind Energy Council, Tech. Rep., 2021.
- [2] S. P. Mulders, T. G. Hovgaard, J. D. Grunnet, and J.-W. van Wingerden, "Preventing wind turbine tower natural frequency excitation with a quasi-lpv model predictive control scheme," *Wind Energy*, vol. 23, no. 3, pp. 627–644, 2020.
- [3] M. Lara, J. Garrido, M. L. Ruz, and F. Vázquez, "Adaptive pitch controller of a large-scale wind turbine using multi-objective optimization," *Applied Sciences*, vol. 11, no. 6, 2021.
- [4] M. L. Shaltout, Z. Ma, and D. Chen, "An Adaptive Economic Model Predictive Control Approach for Wind Turbines," *Journal of Dynamic Systems, Measurement, and Control*, vol. 140, no. 5, 12 2017, 051007.
- [5] A. Pamososuryo, Y. Liu, T. Hovgaard, R. Ferrari, and J. Van Wingerden, "Individual pitch control by convex economic model predictive control for wind turbine side-side tower load alleviation," *Journal of Physics: Conference Series*, vol. 2265, no. 3, 2022, 2022 Science of Making Torque from Wind, TORQUE 2022.
- [6] J. B. Rawlings, D. Angeli, and C. N. Bates, "Fundamentals of economic model predictive control," in *2012 IEEE 51st IEEE conference on decision and control (CDC)*. IEEE, 2012, pp. 3851–3861.
- [7] T. Faulwasser, L. Grüne, M. A. Müller *et al.*, "Economic nonlinear model predictive control," *Foundations and Trends® in Systems and Control*, vol. 5, no. 1, pp. 1–98, 2018.
- [8] S. Gros, "An economic nmpc formulation for wind turbine control," in *52nd IEEE Conference on Decision and Control*. IEEE, 2013, pp. 1001–1006.
- [9] W. K. Gawronski, *Advanced Structural Dynamics and Active Control of Structures*, ser. Mechanical Engineering Series. New York: Springer-Verlag, 2004.
- [10] J. Jonkman, S. Butterfield, W. Musial, and G. Scott, "Definition of a 5-MW Reference Wind Turbine for Offshore System Development," Tech. Rep. NREL/TP-500-38060, 947422, Feb. 2009.
- [11] T. G. Hovgaard, S. Boyd, and J. B. Jørgensen, "Model predictive control for wind power gradients," *Wind Energy*, vol. 18, no. 6, pp. 991–1006, 2015.
- [12] G. G. J. Ruitkamp, "Modelling and Control of Lateral Wind Turbine Tower Dynamics," Master's thesis, Delft University of Technology, 2021.
- [13] Z. Zhang, S. R. K. Nielsen, F. Blaabjerg, and D. Zhou, "Dynamics and control of lateral tower vibrations in offshore wind turbines by means of active generator torque," *Energies*, vol. 7, no. 11, pp. 7746–7772, 2014.
- [14] E. S. P. Branlard, "Flexible multibody dynamics using joint coordinates and the rayleigh-ritz approximation: The general framework behind and beyond flex," *Wind Energy*, vol. 22, no. 7, pp. 877–893, 2019.
- [15] D. Schlipf, D. J. Schlipf, and M. Kühn, "Nonlinear model predictive control of wind turbines using lidar," *Wind Energy*, vol. 16, no. 7, pp. 1107–1129, 2013.
- [16] S. Boyd, S. P. Boyd, and L. Vandenberghe, *Convex optimization*. Cambridge university press, 2004.